Chemical Engineering Journal 161 (2010) 409–415

Contents lists available at ScienceDirect

Chemical Engineering Journal

journal homepage: www.elsevier.com/locate/cej

Diesel-fuel improver production via novel heterogenized solid-acid catalysts

L. Spadaro[a,b,*], F. Arena[b,a], O. Di Blasi[a], G. Bonura[a], F. Frusteri[a,b]

[a] Istituto di Tecnologie Avanzate per l'Energia "Nicola Giordano" (CNR-ITAE), Via Salita S. Lucia sopra, Contesse n. 5, I-98126 S. Lucia, Messina, Italy
[b] Dipartimento di Chimica Industriale e Ingegneria dei Materiali, Università degli Studi di Messina, Salita Sperone 31, I-98166 S. Agata, Messina, Italy

ARTICLE INFO

Article history:
Received 10 May 2009
Received in revised form 7 August 2009
Accepted 16 August 2009

Keywords:
Silica-*heterogenized* perfluorosulfonic (PFS) acid catalysts
Preparation method
Acid catalyst properties
ZPC measurements
Acetal synthesis

ABSTRACT

Several polymers with ion exchanging groups showing acidic strength comparable with that of "concentrated" sulfuric acid were used to prepare silica-*heterogenized* perfluorosulfonic (PFS) acid catalysts by either incipient wetness impregnation of commercial silicas or sol–gel and precipitation routes. Solid-acid catalysts were probed in the synthesis of acetal at 4 °C and 3 atm in a stirred batch reactor. A systematic analysis of activity data and the acid strength of the various catalysts points out a direct relationship between the *acidic capacity* and catalytic activity, pointing out a minor influence of the strength distribution on the main reaction path.

1. Introduction

Amongst various classes of potential solid-acid catalysts, in recent years a great interest has been focused on acid ion-exchanged polymers, such as Nafion®, especially for fuel cell applications. This type of solid acids are characterized by the presence of fluorosulfonylethoxy acid groups attached to the different lengthy tetrafluoroethylene polymeric chains [1,2]. The fluorine atoms enhance the acid strength of the terminal sulfonic groups to levels comparable with that of pure sulfuric acid.

Actually, strong mineral acids such as H_2SO_4, HF or Lewis-acid catalysts (i.e. anhydrous $AlCl_3$ or BF_3) are in practice used for the synthesis of *high-value* chemicals [3–6]. The employment of these corrosive compounds is associated with a number of environmental problems [5,6], such as the necessary treatment of hazardous/toxic waste products. Then, environmental and economic reasons [5,6], impose the adoption of cleaner and more selective process technologies deserving the replacement of homogeneous processes with more safe heterogeneous catalytic technologies based on the employment of strong solid-acid catalysts [7]. However, the use of "pure" perfluorosulfonic acid polymers is generally limited by an intrinsic low surface availability reflecting in poor process yields [8].

The acid-catalyzed synthesis process of 1,1-*di*-ethoxyethane (acetal), an important organic compound indicated as suitable "cetane number" (CN) *"improvers"* for diesel fuel [9–11], is the typical example of industrial process still carried out in the presence of strong liquid inorganic acids [12]. Although zeolites and functionalized silica (by addition of sulfonic acid groups) were found to catalyze many organic reactions [13–21], only few articles have addressed the use of stable and selective solid-acid catalysts for the acetal manufacture instead of mineral acids [22,23]. In particular, the feasibility of the acetal synthesis through the employment of catalytic heterogeneous systems has been documented [23]. Probing a series of different acidic systems (zeolite, modified clay and sulfonic ion exchange resins), Capeletti et al. did not observe "a clear relationships between activity and the amount of acidity, or the physical properties of the catalysts" [23].

Therefore, the present work aims to shed lights into the acidic properties of different acid perfluorosulfonic (PFS) systems "heterogenized" by the insertion of silica carriers using different preparation techniques. A systematic evaluation of the catalytic pattern of the various systems outlines basic *acidity–activity* relationships in the synthesis of acetal.

2. Experimental

2.1. Materials

Different loaded (6–40 wt%) acid perfluorosulfonic-*silica* catalysts (PFS-SiO_2), were synthesized either by incipient wetness impregnation or sol–gel precipitation routes [24], according to the following procedures.

* Corresponding author at: Istituto di Tecnologie Avanzate per l'Energia "Nicola Giordano" (CNR-ITAE), Via Salita S. Lucia sopra, Contesse n. 5, I-98126 S. Lucia, Messina, Italy. Tel.: +39 090 624238; fax: +39 090 624247.
E-mail address: lorenzo.spadaro@itae.cnr.it (L. Spadaro).

1385-8947/$ – see front matter © 2009 Elsevier B.V. All rights reserved.
doi:10.1016/j.cej.2009.08.013

Table 1
List of the studied catalysts.

Code	[a]Polymer loading (wt%)	[b]EW	S.A.$_{BET}$ ($m^2\ g^{-1}$)	Pore diameter (Å)
6A-LM50	6.1	n.a.	120	198
12A-LM50	11.8	n.a.	113	176
18A-LM50	17.6	n.a.	107	146
24A-LM50	23.6	n.a.	99	132
30A-LM50	29.5	n.a.	95	129
30A-M5	29.5	n.a.	187	111
30A-F5	29.3	n.a.	571	53
40A-SOL[c]	39.1	n.a.	68	36
100A[d]		810	<1	–
12B-LM50	11.2	n.a.	116	180
18B-LM50	17.1	n.a.	103	157
24B-LM50	24.2	n.a.	98	139
30B-LM50	29.3	n.a.	97	125
100B[d]		920	<1	–
12C-LM50	12.2	n.a.	118	191
18C-LM50	18.1	n.a.	111	165
24C-LM50	23.7	n.a.	98	133
30C-LM50	30.6	n.a.	93	119
100C[d]		1050	<1	–
12D-LM50	12.2	n.a.	111	171
18D-LM50	17.8	n.a.	107	152
24D-LM50	23.7	n.a.	99	137
30D-LM50	28.3	n.a.	96	127
100D[d]	6.1	935	<1	–

[a] Estimated by TG analysis and from silica/sulfur ratio carried out by XRF elemental analysis.
[b] Equivalent weight (EW) of Hyflon® copolymers as declared by producer and confirmed by CHNS analysis (as ratio between carbon and sulfur).
[c] Prepared by sol–gel (sg) method.
[d] PFS-polymer foil as obtained by solvent evaporation.

2.1.1. Incipient wetness catalyst

Catalysts were prepared by the stepwise addition of several not commercial Hyflon® Ion perfluorosulfonic alcoholic solutions (*Solvay Solexis Co.*) to commercial SiO_2 carriers. The various solutions of Hyflon® Ion PFS copolymers (signed as type-A–D) were characterized by a different *equivalent weight* (EW), ranging from 810 to 1050 (g/–HSO_3 equiv.) as reported in Table 1, resulting thus in a higher acidity than that of the commercial Nafion®1100. Three different commercial silica samples with different *Surface Area* (S.A.), namely, silica *"LM50"* (*Fumed silica*, *Cab-O-Sil division*; S.A. = 120 $m^2\ g^{-1}$), silica *"M5"* (*Fumed silica*, *Cab-O-Sil division*; S.A. = 200 $m^2\ g^{-1}$) and silica *"F5"* (*Akzo*, *Chemical division* A.S. = 600 $m^2\ g^{-1}$), were used as support. Hyflon® Ion copolymer solutions were added to *SiO_2*-supports until incipient wetness and then dried at 60 °C for 30 min. This procedure was repeated until the designed amount of polymer was loaded on the support. After impregnation all the samples were treated in air at 120 °C for 2 h.

2.1.2. Sol–gel precipitated catalyst

Sol–gel precipitated catalyst was prepared employing the isopropanolic solution of Hyflon® *type*-A copolymer and a commercial solution (*99.99% Carlo Erba products*) of tetraethylorthosilicate [$Si(EtO)_4$], according to the procedure elsewhere described [24].

The list of the studied samples is presented in Table 1.

2.2. Methods

2.2.1. Thermogravimetry and differential scanning calorimetry (TGA–DSC)

The amount of PFS-polymer was determined by TGA–DSC using a NETZSCH Simultaneous Thermal Analysis Instrument STA 409 C.

2.2.2. X-ray fluorescence spectrometry (XRF)

The analytical composition of catalysts ware confirmed by XRF analysis using a *BRUKER AXS - S4 Explorer* spectrometer, equipped with a Rhodium X-ray source (Rh anode and 75 μm Be-window).

2.2.3. CHNS analysis

The *equivalent weight* (EW) of unsupported PFS-polymers were evaluated by a CHNS-O *Flash EA^{TM} 1108 THERMO FINNIGAN*.

2.2.4. X-ray diffraction (XRD)

Analysis of powdered catalysts was carried out using a *Philips X-Pert* diffractometer operating with Cu Kα radiation at 40 kV and 30 mA. Modelling of XRD spectra has been performed by deconvolution analysis of experimental profiles by a linear combination of Gaussian components, using the "*PeakFit v4*" software package (*Jandel Scientific*) [25].

2.2.5. Scanning electron microscopy (SEM)

Analyses have been carried out using a *Jeol 5600 LV* microscope operating with an accelerating voltage of 20 kV. SEM micrographs were taken after samples coating by gold sputtering.

2.2.6. Titration

The Brönsted acidity was estimated electrochemically by Zero Point Charge (ZPC) measurements, according to the procedure elsewhere described [26].

2.2.7. Catalytic tests

Catalytic tests in the acetal synthesis were performed at 4 °C and a total pressure of 3 atm, using a 100 cm^3 batch reactor containing 0.05 g of catalyst and 60 mL of a reactant mixture of acetaldehyde/ethanol (1:2) stirred at 2000 rpm. Toluene (2 mL) was used as internal standard for GC analysis. The reaction temperature (4 ± 0.1 °C) was controlled by a thermocouple inserted into the slurry, while reagents and products were analysed by using a *HP 5890* gas chromatograph equipped with a packed-column (6.6% of *Carbowax/carbograph*; *l* = 20 m; *d* = 1/8″; *Alltech products*) connected to a FID detector.

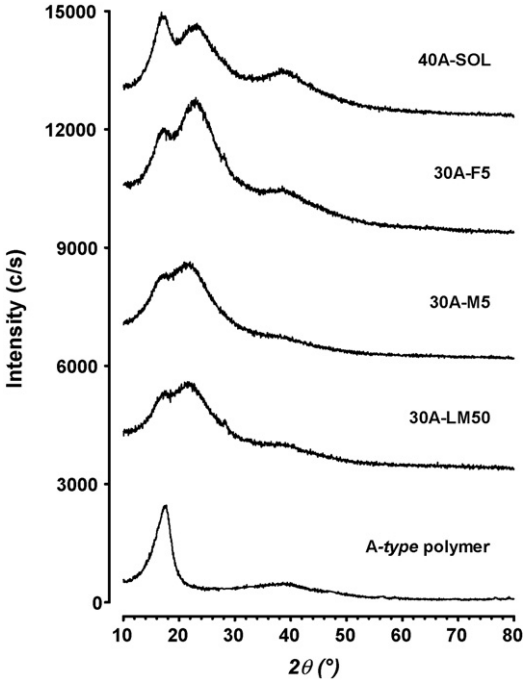

Fig. 1. X-ray diffraction patterns of the highly loaded *type*-A catalysts and reference unsupported PFS-polymer (*type*-A).

3. Results

3.1. Structural properties

As reported in Table 1, impregnated catalysts with an analogous loading of *type*-A polymer (30%) are characterized by marked differences in the texture (*surface area and pore diameter*), related to the physical properties of the various commercial silica carriers. The sample 30A-F5 features the highest surface area (S.A.) equal to 600 $m^2\ g^{-1}$, while the samples 30A-M5 and 30A-LM50 have surface area values of ca. 200 and 100 $m^2\ g^{-1}$, respectively. Moreover, all the catalysts prepared by incipient wetness impregnation feature a similar *pore size distribution*, characterized by the prevalence of mesopores with an average diameter (50–200 Å) fairly dependent either on loading or type of polymer. Due to a higher content of *type*-A polymer (40%), the catalyst 40A-SOL shows the lowest surface area (70 $m^2\ g^{-1}$) and an average pore diameter smaller than 40 Å.

The XRD patterns of the highly loaded *type*-A catalysts, are compared in Fig. 1. All the samples display rather broad and poorly resolved XRD lines in 2θ range 10–45°, likely coming from the convoluted signals of amorphous (2θ = 16.0°) and crystalline (2θ = 17.5°) phases relative to polyfluorocarbon chains [25] and the amorphous (2θ = 21.5°) phase of silica. In particular, the bare *type*-A polymer displays a rather symmetric XRD peak in the 2θ range 10–20°, while all the supported catalysts feature a much broader diffraction pattern (10–30°) characterized by two more or less resolved maxima, whose relative intensity depends upon the silica carrier and polymer loading.

The SEM images of samples 30A-F5, 30A-LM50 and 40A-SOL, shown in Fig. 2, indicate that both preparation method and support texture are decisive for the catalyst morphology. Namely, the catalyst 30A-F5 (Fig. 2c) is characterized by the presence of irregular small particles (<2 m), where the perfluorosulfonic phase is hardly, if any, distinguishable. On the contrary, SEM image of sample 30A-LM50 (Fig. 2b) shows a more regular structure consisting of aggregates with an average size of ca. 20 μm featuring a *sponge*-like architecture, likely due to "*over saturation*" of pores with consequent growth of a *multi*-layer perfluorosulfonic phase on the low surface area of LM50-silica support (S.A. ≈100 $m^2\ g^{-1}$).

At least, the morphology of the 40A-SOL sample is substantially different (Fig. 2a), showing a homogeneous and well consolidated PFS-SiO_2 structure, likely consisting of a polymeric substrate (perfluorosulfonic membrane) filled by small grains of amorphous silica.

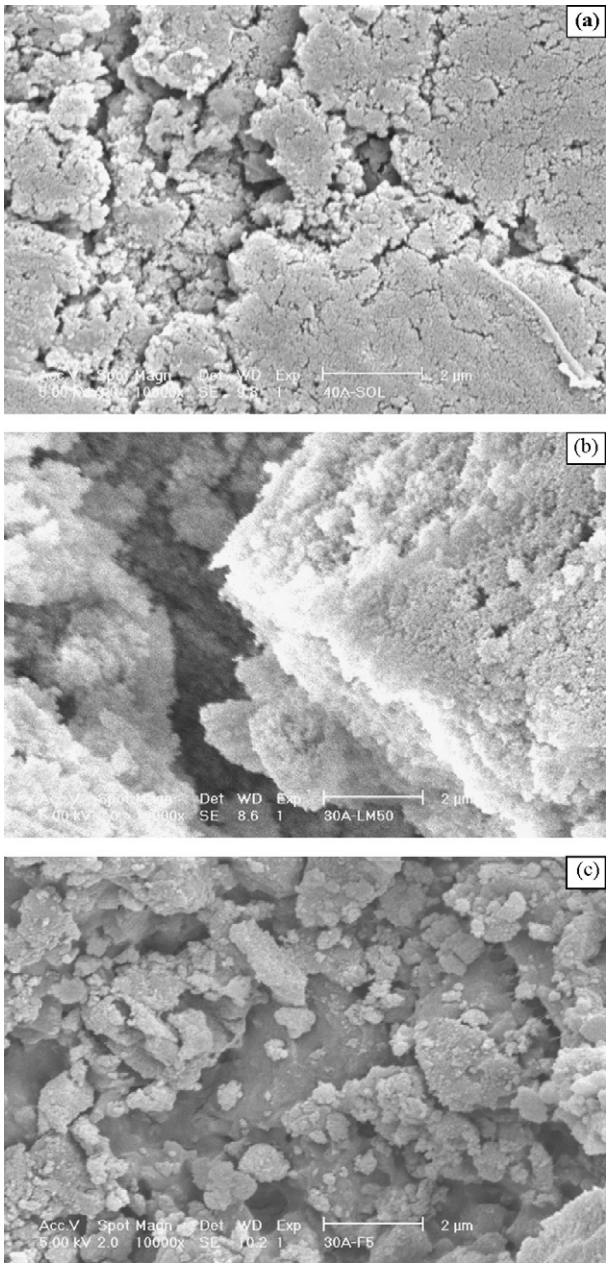

Fig. 2. SEM pictures of samples 40A-SOL (a), 30A-LM50 (b) and 30A-F5 (c), (×10,000).

3.2. Acidic properties

Titration curves of the *type*-A/LM50-SiO_2 catalysts are shown in Fig. 3A, while the data relative to the acidic capacity of the various catalysts are summarised in Table 2 either in terms of proton equivalent *per* gram of catalyst (μequiv. $H^+\ g_{catalyst}^{-1}$) or gram of polymer (mequiv. $H^+\ g_{polymer}^{-1}$). Namely, all the studied systems possess an acidic capacity ranging from 70 to 460 μequiv. $H^+\ g_{catalyst}^{-1}$

Table 2
Acidity of the studied catalysts.

Code	[a] $e/w_{(ZPC)}$ μequiv. $H^+\ g_{catalyst}^{-1}$	[b] $e/w_{(ZPC)}$ mequiv. $H^+\ g_{polymer}^{-1}$	[c] $\Delta(e/w)$ mequiv. $H^+\ g_{polymer}^{-1}$
6A-LM50	73	1.151	−0.084
12A-LM50	154	1.155	−0.080
18A-LM50	185	1.162	−0.073
24A-LM50	283	1.175	−0.060
30A-LM50	354	1.178	−0.057
30A-M5	351	1.171	−0.064
30A-F5	348	1.163	−0.072
40A-SOL	458	1.145	−0.090
12B-LM50	147	0.930	−0.157
18B-LM50	178	1.111	0.024
24B-LM50	239	1.158	0.071
30B-LM50	310	1.025	−0.062
12C-LM50	125	0.961	0.009
18C-LM50	148	0.888	−0.064
24C-LM50	191	0.874	−0.078
30C-LM50	255	0.925	−0.027
12D-LM50	144	1.153	0.083
18D-LM50	171	1.110	0.040
24D-LM50	229	1.020	−0.050
30D-LM50	301	1.002	−0.068

[a] Brönsted acid capability, expressed in term of μequiv. of proton (H^+) *per* gram of catalyst, from ZPC measurements.
[b] Brönsted acid capability, expressed in term of mequiv. of proton (H^+) *per* gram of polymer, from ZPC measurements.
[c] Difference between the theoretical proton (H^+) contents by PFS-polymer loading and that estimated by ZPC measurements.

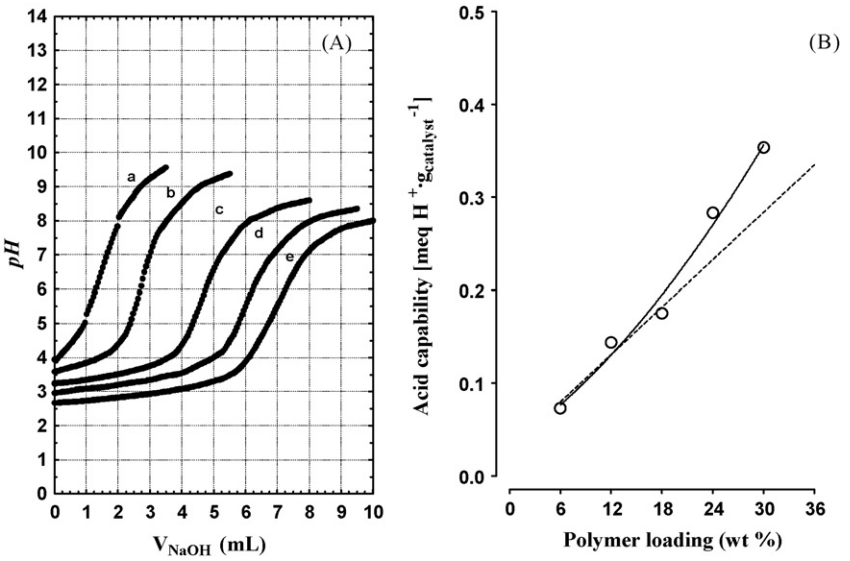

Fig. 3. (A) Titration curve of samples 6A-LM50 (a), 12A-LM50 (b), 24A-LM50 (d) and 30A-LM50 (e) and (B) relationship between acidic capacity of LM50-*silica* supported samples and polymer (*type*-A) loading.

and closely dependent on the amount of polymer (6–40 wt%) and relative acidity. In fact, considering the influence of loading on the acid capacity of the hybrid systems, a progressive rise of the acidity with the polymer loading is observed in the whole range (6–30 wt%), as shown in Fig. 3B. Then, in spite of an acid strength of Hyflon® similar to that of pure sulfuric acid, the profiles of the titration curves account for a weak-type acid behaviour of supported polymer [26], as shown in Fig. 3A. In other words, the dispersion of the PFS-polymers on carriers reduces the acid strength of the perfluorosulfonic phase, probably because of the interaction of the acidic groups with the surface hydroxyls of the support. In fact, the negative effect of the carrier on the acid-strength results stronger at lower loadings (<18%), as indicated by the straight-line increase of acidity with the loading, much less pronounced in comparison to the exponential growth observed at "high coverage". This likely mirrors the weakening of the proton–hydroxyl interaction resulting thus in a superior proton-donor capacity, Fig. 3B.

Table 3
Catalytic activity data at 30 min of reaction time (*T*, 4 °C; *P*, 3 atm).

Catalysts	$X_{acetaldehyde}$ (%)	Acetal productivity (mol h^{-1} $g_{catalyst}^{-1}$ L_{slurry}^{-1})	Site Time Yield (mol h^{-1} mequiv. $(H^+)^{-1}$ L_{slurry}^{-1})
6A-LM50	2.5	5.9	80.8
12A-LM50	5.5	13.1	85.1
18A-LM50	7.1	16.1	87.0
24A-LM50	10.9	26.1	92.2
30A-LM50	14.5	34.8	98.6
30A-M5	14.1	33.8	96.3
30A-F5	13.5	32.7	94.0
40A-SOL	15.0	35.9	78.4
12B-LM50	5.1	12.2	83.0
18B-LM50	6.2	15.0	84.3
24B-LM50	8.8	21.2	88.7
30B-LM50	12.8	30.8	99.4
12C-LM50	4.3	10.4	83.2
18C-LM50	5.2	12.5	84.5
24C-LM50	7.1	17.1	89.5
30C-LM50	9.8	23.6	92.5
12D-LM50	5.0	11.9	82.6
18D-LM50	6.1	14.5	84.8
24D-LM50	8.5	20.3	88.6
30D-LM50	12.3	29.4	97.7

3.3. Catalytic activity

The catalytic synthesis of acetal in the presence of heterogenized perfluorosulfonic systems leads to the exclusive formation of acetal. On the other hand, no traces of PFS in the reacting solution, due to leaching phenomena, were detected by NMR [27], while any significant activity loss was recorded during 24 h endurance tests. In addition, the used-catalysts showed an unchanged performance at least in three catalytic tests (data not reported for the sake of brevity). Then, activity data at 30 min of reaction time, using a catalyst/reagents weight ratio of 1/900 are summarised in Table 3, in terms of *acetaldehyde conversion* ($X_{acetaldehyde}$, %),

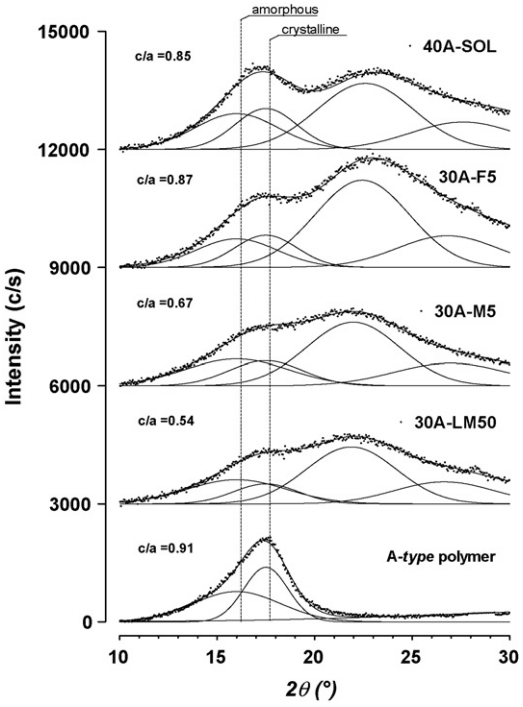

Fig. 4. Deconvolution analysis of X-ray diffraction peaks of the highly loaded *type*-A catalysts and reference unsupported PFS-polymer (*type*-A).

acetal productivity (mol h^{-1} $g_{catalysis}^{-1}$ L_{slurry}^{-1}) and *Site Time Yield* (mol h^{-1} mequiv.H^{+-1} L_{slurry}^{-1}). In agreement with a higher *Brönsted*'s acid capacity a superior catalytic performance is found for the catalysts with higher perfluorosulfonic loading (30–40%), denoted by the highest acetaldehyde conversion (ca. 13–15%). As a rule, the conversion increases with the acid strength of catalysts, irrespective of the type of perfluorosulfonic polymer (A–D). Namely, for highly loaded catalysts the activity scale in terms of *acetal productivity* results to be as follows (Table 3):

40A-SOL > 30A-LM50 > 30A-M5 > 30A-F5 > 30B-LM50

> 30D-LM50 > 30C-LM50,

in a good agreement with the "acid site density" (μequiv. H^+ $g_{catalyst}^{-1}$) data in Table 2. While in term of *Site Time Yield* (STY) the overall activity order is significant far from that of above *productivity*, resulting as follows (Table 3):

30B-LM50 > 30A-LM50 > 30D-LM50 > 30A-M5 > 30A-F5

> 30C-LM50 > 40A-SOL

This finding points out also some influence of catalyst structure. In particular, the textural properties of SiO_2 support seem to play a key role on catalytic performance. In fact, an appreciable decrease in the acetaldehyde conversion was observed to be associated with the increase in catalyst surface area, mirroring thus a noticeable decrease of the *Site Time Yield* (STY).

4. Discussion

As shown in Fig. 4, the concomitant presence of amorphous and crystalline phases of polyfluorocarbon chains have been evaluated by deconvolution analysis of XRD pattern of samples 40A-SOL, 30A-F5, 30A-M5, 30A-LM50 and "copolymer-A film" [25]. A rise in *surface area* implies an almost proportional growth of crystalline PFS chain, being the ratio between the peak area of crystalline and amorphous phases "c/a" rising from 0.54 to 0.87 at the increasing of S.A. from 100 m^2 g^{-1} (30A-LM50) to 570 m^2 g^{-1} (30A-F5).

The deconvolution of XRD spectra of unsupported perfluorosulfonic polymer (reference *type*-A) provides a "c/a" value equal to 0.91, very close to that of 0.87 found for 30A-F5 cat-

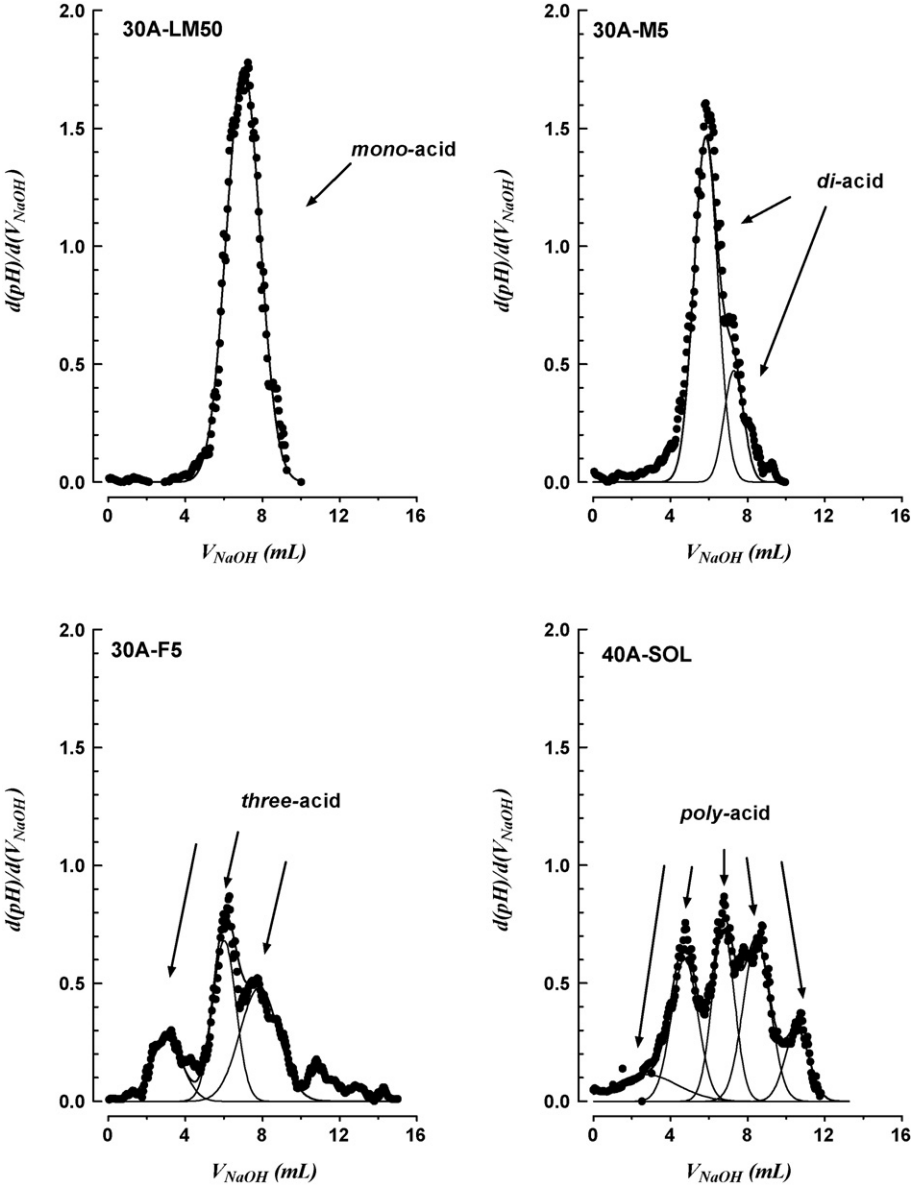

Fig. 5. Deconvolution analysis of first derivative titration curves of catalysts.

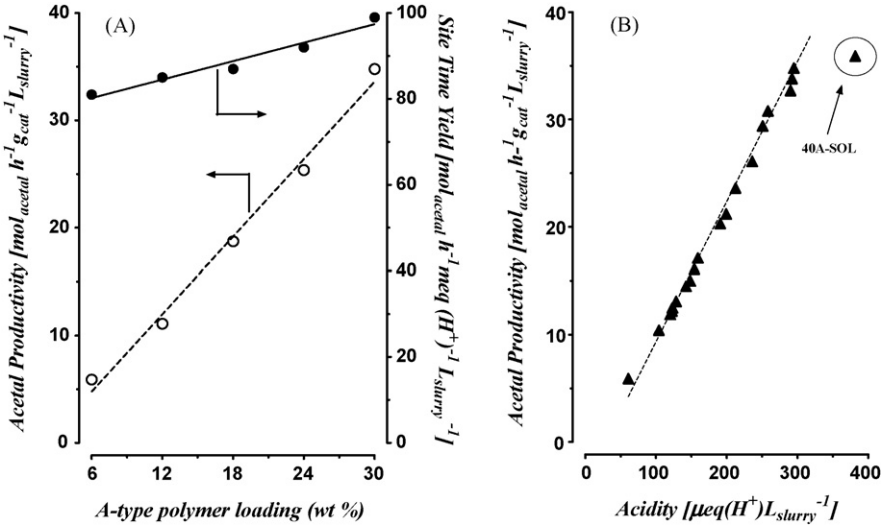

Fig. 6. Synthesis of acetal at 4 °C and 3 atm. (A) Acetal productivity and STY of LM50-*silica* supported samples *vs.* polymer (*type*-A) loading and (B) acetal productivity of various catalysts *vs.* acidity.

alyst and 0.85 of the 40A-SOL sample prepared by the *sol–gel* method.

These findings suggest that the upper grade of crystallinity of the PFS phase for the samples 30A-F5 and 40A-SOL is a consequence of both the textural properties of the SiO_2 support (e.g., abundance and volume of pores) and preparation method (e.g., *in situ* formation of small sized inorganic particles). In fact, it is known that the crystalline nature of the PFS polymers arises from *ordered* packing (straight-elongation) of the polyfluorocarbon back-bond chains ($[\sim(CF_2–CF_2)\sim]_n$), which arrange in a "reversed-micelle" structure [28]. Then, for the bare membrane the formation of such micelle-*type* structures would occur in strong polar (dielectric constant > 10) solvents, whereas for composite membranes the same process takes place at the surface of adsorbing material/support [28]. It is generally recognised that a strong "compaction" of the recast copolymer produces a significant straight-elongation and ordering of the polyfluorocarbon chain with a consequent increase of the crystalline character of the PFS polymers [29]. Similarly, capillarity effects could enable the formation of reversed-micelle structures in *nano*-composite membranes as a consequence of the impregnation of small sized microporous oxide particles [28]. However, it must be pointed out that an increasing fraction of the crystalline phase could also be stabilised by subsequent thermal treatments during preparation ($T > 100$ °C) of either composite or bare membranes [30].

Then, SEM images of samples 30A-F5 and 40A-SOL (Fig. 2) show that in the case of the former sample (30A-F5) at higher surface area (S.A.), the polymeric phase result to be highly dispersed on the surface of the F5 silica support. On the contrary, in the case of the latter catalyst prepared by *sol–gel* method (40A-SOL), small sized particles of silica (<0.1 μm) appear *"dispersed-organized"* into a polymeric template.

Moreover, ZPC measurements (Fig. 4) show that the catalysts characterized by a stronger PFS-SiO_2 interaction (30A-F5 and 40A-SOL), due to the superior dispersion of the perfluorosulfonic phase, behave similar to mineral *poly*-acids characterized by a different acid strength. In fact, the differential analysis of titration curves reveals the presence of several maxima that prove the occurrence of *multi*-equilibrium steps due to weak-acid/strength-base titration reactions, as shown in Fig. 5. Whereas, the catalysts with lower surface area (S.A.) and dispersion of the perfluorosulfonic phase, feature a titration pattern denoting an almost *mono*-acidic behaviour, Fig. 5.

Therefore, the presence of multi-equilibrium indicates some role of the SiO_2 support that could induce some electronic effect on the PFS-polymer chain and/or induces some mass transfer diffusion phenomena, hindering the protons mobility of sulfonic acidic groups [$–SO_3H$]. In other words, the interaction of polymer molecules with the carrier surface could lead to sulfonic acid groups characterized by a different acid strength, explaining the different behaviour of heterogenized perfluorosulfonic catalysts (Table 3), previously ascribed to the different surface area and active phase dispersion. Therefore, these findings indicate a direct relationship between surface "acidity" and catalytic efficiency, in the sense that a superior protons mobility drives a higher performance in the synthesis of acetal.

Catalytic activity data in the acetal synthesis, both in terms of productivity and STY, plotted in Fig. 6A as a function of the copolymer (A-type) loading, depict in fact fairly reliable straight-line relationships diagnostic of a full availability of sulfonic acidic groups at the catalyst surface. This could be the consequence of the preferential interaction of the polymer with the silica surface through the fluoride group by hydrogen-like bonds. Then, far away from equilibrium conditions, the reaction kinetics depend almost linearly upon the *Brönsted* acidity according to an almost *straight*-line increase in acetal productivity with the acidity concentration of the reaction medium, until a value of ca. 300 μequiv. L_{slurry}^{-1} (Fig. 6B). In other words the acid strength plays a minor influence on the main reaction path because of the easy mobility of protons in the reaction medium.

The deviation from the linearity of the sample 40A-SOL stems from a weaker acidity (Fig. 5) and, mostly, by the fast attainment of equilibrium imposing a thermodynamic constraint to the net reaction rate:

$$2C_2H_5OH + CH_3CHO \overset{H^+}{\rightleftarrows} (C_2H_5O)CHCH_3 + H_2O$$

Since its overwhelming acidic capacity (Table 2), then, the catalysts 40A-SOL attains the equilibrium conversion just after 30 min of reaction time with relative thermodynamic limitations (Table 3 and Fig. 6). Anyhow, the highest acetal productivity values (33–36 mol h^{-1} $g_{catalyst}^{-1}$ L_{slurry}^{-1}) obtained on samples 30A-F5, 30A-M5, 30A-LM50 and 40A-SOL using a catalyst/reagents ratio of 1/900 (wt/wt), are higher by ca. two orders of magnitude than those reported in the literature using different type of solid-acid catalysts [23].

5. Conclusions

The main results of this work can be synthesized as follows:

- The *heterogenization* of PFS acid polymers using different SiO_2 carriers and preparation techniques does not affect the acidic properties of the starting polymers.
- A very significant improvement in the surface area allows for a full availability of the sulfonic acidic groups, enabling a remarkable performance of *Perfluorosulfonic-SiO_2* catalysts in the liquid-phase synthesis of acetal.
- *Perfluorosulfonic-SiO_2* systems result very active and selective towards the production of acetal, denoting also a good mechanical and chemical stability under typical process conditions (*T*, 4 °C; *P*, 3 atm).
- A *straight*-line relationship between acetal productivity and catalyst acidic capacity signals a minor influence of the strength distribution on the main reaction path.

Acknowledgement

This work has been realized with the technical and financial support of *Solvay-Solexis* Company (R&D Department, Bollate (Milan) – Italy) in the framework of the research contract with CNR-ITAE.

References

[1] G.A. Olah, NATO ASI Ser. C 444 (1994) 305.
[2] M.A. Harmer, W.E. Farneth, Q. Sun, Adv. Mater. 10 (1998) 1255.
[3] G.A. Olah, Friedel–Crafts and Related Reactions, Wiley, New York, 1974.
[4] H. Szmant, Organic Building Blocks of Chemical Industry, Wiley, New York, 1989.
[5] R.A. Sheldon, Chem. Ind. (1997) 12.
[6] R.A. Sheldon, H. Van Bekkum, Fine Chemicals through Heterogeneous Catalysis, Wiley–VCH, Weinheim, 2000.
[7] A. Corma, H. Garcia, Chem. Rev. 103 (2003) 4307.
[8] M. Alvaro, A. Corma, D. Das, V. Fornés, H. García, J. Catal. 231 (2005) 48.
[9] J. Peckham, Diesel likeliest option for high-mileage car says NRC, in: Fuels and Lubricants, Hart's Fuels and Lubes SAE Show Special, Hart Publication, Potomac, MD, 1997.
[10] K. Owen, T. Coley, Diesel fuel additives, in: Automotive Fuels Reference Book, 2nd ed., 1995, p. 503.
[11] L.N. Allard, N.J. Hole, G.D. Webster, T.W. Ryan, D. Otto III, A. Beregszazy, C.W. Fairbridge, J. Cooley, K. Mitchell, E.K. Richardson, N.G. Elliot, D.J. Rickeard, SAE Tech. Pap. Ser. 971636 (1997) 45.
[12] M. Kaufhold, M. El-Chahawi. Pat. DE 44 04 515 A1 (1995) to Huls AG, Germany.
[13] A. Corma, M.J. Climent, H. García, J. Primo, Appl. Catal. 49 (1989) 109.
[14] R. Fang, G. Harvey, H.W. Kouwenhoven, R. Prins, Appl. Catal. Gen. A 130 (1995) 67.
[15] K. Garre, D. Akporiaye, J. Mol. Catal. A 109 (1996) 177.
[16] K. Smith, Z. Zhenhua, P.K.G. Hodgson, J. Mol. Catal. A 134 (1998) 121.
[17] Y. Ma, W. Wang, W. Jiang, B. Zuo, Appl. Catal. Gen. A 165 (1997) 199.
[18] D. Das, S. Cheng, Appl. Catal. Gen. A 201 (2000) 159.
[19] Q.L. Wang, Y. Ma, X. Ji, Y. Yan, Q. Qiu, Chem. Commun. (1995) 2307.
[20] R.D. Badley, W.T. Ford, J. Org. Chem. 54 (1989) 5437.
[21] G. Olah, P.S. Iyer, G.K. Surya Prakash, Synthesis (1986) 513.
[22] J. Andrade, D. Arntz, M. Kraft, G. Prescher. Pat. DE 34 03 426 A1 (1985), Degussa AG, Germany.
[23] M.R. Capeletti, L. Balzano, G. de la Puente, M. Laborde, U. Sedran, Appl. Catal. Gen. A 198 (2000) L1.
[24] M.A. Harmer, W.E. Farneth, Q. Sun, J. Am. Chem. Soc. 118 (1996) 7708.
[25] P.L. Antonucci, A.S. Aricò, P. Cretì, E. Ramunni, V. Antonucci, Solid State Ionics 125 (1999) 431.
[26] F. Frusteri, L. Spadaro, C. Beatrice, C. Guido, Chem. Eng. J. 134 (2007) 239–245.
[27] N.J. Bunce, S.J. Sondheimer, C.A. Fyfe, Macromolecules 19 (1986) 333.
[28] M. Uchida, Y. Aoyama, N. Eda, A. Ohta, J. Electrochem. Soc. 142 (1995) 463.
[29] F.W. Billmeyer, Textbook of Polymer Science, 3rd ed., Wiley-Interscience Publication, 1984, p. 276.
[30] G. Alberti, M. Casciola, Annu. Rev. Mater. Res. (2003) 129.